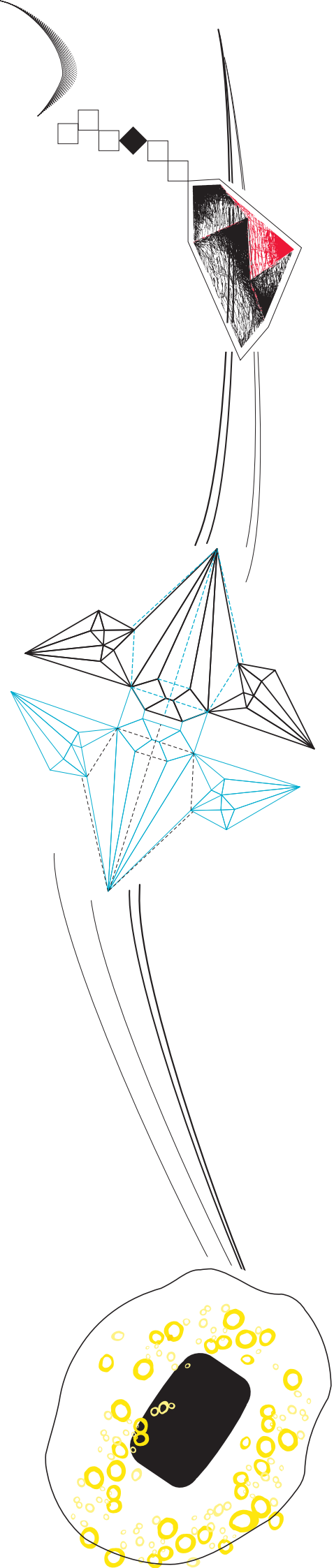

UNIVERSITY OF TWENTE.

Faculty of Electrical Engineering,
Mathematics & Computer Science

Control Surface Waves by Modifying Surface Properties of a Microstrip Patch Antenna Array

Stephan de Louw

MSc. Thesis
April 2017

Supervisors Daily
dr. ir. G. H. C. van Werkhoven
MSc. D. Alvarez Menendez

Supervisors Committee
dr. ir. M. J. Bentum
prof. dr. ir. ing. F. B. J. Leferink
prof. dr. ir. F. E. van Vliet
dr. ir. G. H. C. van Werkhoven

Telecommunication Engineering Group
Faculty of Electrical Engineering,
Mathematics and Computer Science
University of Twente
P.O. Box 217
7500 AE Enschede
The Netherlands

Summary

Not publicly accessible.

Contents

List of Abbreviations

AF	Array Factor
CRLH	Composite Right/Left-Handed
COF-SIM	Coupled Free-Space - Surface IMpedance
EBG	Electromagnetic Band Gap
FSS	Frequency-Selective Surfaces
HIS	High-Impedance Surface
HFSS	High Frequency Structure Simulator (product name)
LW	Leaky Wave
PCB	Printed Circuit Board
PW	Plane Wave
RF	Radio Frequency
SW	Surface Wave
TL	Transmission Line
TM	Transverse Magnetic

Chapter 1

Surface Waves; an Introduction

1.1 Intro

This research is done as the final part of the master Electrical Engineering studied at the University of Twente. The research is done externally at Thales Netherlands, at the branch located in Hengelo, responsible for naval, logistics, and air defence systems. Most of there systems rely on radar, and therefore this thesis is also connected to radar systems.The thesis investigates a very small part in the whole radar system and focuses on the antenna panel consisting of microstrip patch antennae. One of the possible ways to improve the antenna patterns of the radar is by the reduction of the interferences causes in the patterns by Surface Waves (SWs). In this project a solution is investigated for a X-band system ($8.0 - 12.0$ GHz), although the theory is applicable for different frequencies.
This chapter, Chapter 1, gives some background information about SWs, how they can be reduced and the chapter ends with the report organization.

1.2 Background

1.2.1 Surface Waves in Microstrip Patch Antenna Array

Nowadays many radar systems are based on array antennas since they have clear benefits over classical (reflectors) based systems. For example fast electric beam steering and adaptivity of the used beam shapes. In one array antenna, the antenna pattern is not formed by a single radiating element but by the coherent combination of all elements in which weighting factors can be applied. These factors enables beam steering and/or beam shaping.The resulting antenna beam pattern is (to some degree of accuracy) given by the Array Factor (AF) multiplied with the averaged element pattern. By using certain weigh factors for each element an antenna

pattern is created which is suitable for a radar application, with a main lobe and low side lobes. Unfortunately the side lobes have still enough energy and under some conditions they are able to propagate along the surface, known as surface waves.
Since surface waves are propagating waves, propagating along a surface, they can increase the coupling of energy between array elements, so called mutual coupling. Mutual coupling is an unwanted limiting factor of array antennas, affecting its radiation pattern and scan behaviour. But this is not the only problem, the SW also brings Radio Frequency (RF) power to the antenna's panel edge. When the edge is reached it starts to re-radiate in the same plane as the radiation occurs. The fields from the edge add up constructive or destructive with the primary element pattern. These effects are shown in the coming part.

Figure 1.1 shows the case where a single element is transmitting and an additional source represents the panel's edge. This additional source is located at 5λ, power -20 dB with respect to the primary element, and 10λ, -30 dB and add up destructive (90° degree out of phase).
From the Figure a trend is visible, less power for the additional source leads to a smaller ripple compared to single element pattern. Further power decreasing lead to a negligible effect on the main element pattern. This is the case for a single element and edge radiation. However in an antenna array each element has a different distance to the edge and so the interference is different. This can cause element patterns in the array and change the array beam pattern.

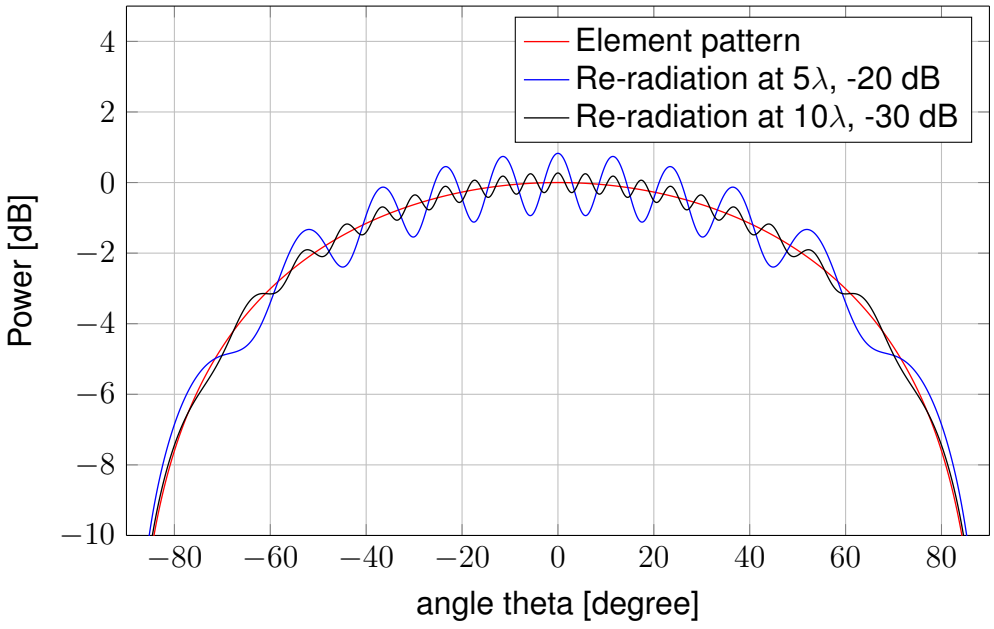

Figure 1.1: Influence of re-radiated energy on the element pattern.

Figure 1.1 shows the influence on one element but does not show the impact on the radiation pattern in a linear 1D array. Assume N elements with an inter element spacing equal to d_1. Without the re-radiation the field pattern expressed in power is represented by [1]:

$$P(\theta) = \sum_{n=1}^{N} w_n e^{j(n-1)(kd_1 \cos\theta+\beta)} * f_e(\theta) \tag{1.1}$$

where w_n is weighting factor that depends on the element, k represents the wavenumber, θ the scan angle, β is the phase different between the elements and $f_e(\theta)$ is the radiation pattern of a single element. Due to the re-radiation an additional term is required:

$$P(\theta) = \sum_{n=1}^{N} w_n e^{j(n-1)(kd_1 \cos\theta+\beta)} * f_e(\theta) + w_{sw} e^{j(n-1)(k(d_1+d_2) \cos\theta+\beta)} \tag{1.2}$$

where d_2 is the additional distance seen from the n-th inspected element toward the location where the re-radiation occurs and is responsible for an additional phase change. The weighting function w_{sw} is:

$$w_{sw} = \kappa e^{jkd_2} \tag{1.3}$$

where κ is a constant, representing the amplitude of the SW. Concluded each individual element pattern is affected by re-radiation, and so the total radiation pattern is influenced. When the re-radiated power becomes stronger the interference level is increased.

In the previous part the effects of SWs on the element pattern was addressed and some first steps were made to a 1D array. The coming part extends this part and show the radiation pattern for two radiating patch antennas and the effect of SWs. Sievenpiper *et al.* [2] measured the radiation pattern for two radiating elements and changes the surfaces to affect SWs. The first surface consist of a metal plane (conducting) where the second surface is made from a materiel that creates a high-impedance surface. The high-impedance surface does not support SW propagation and so no re-radiation occurs. The used configuration is shown in Figure 1.2.

Figure 1.2: Patch antenna above: (a) metal plane (b) high-impedance plane.

The resulting radiation patterns are shown below.

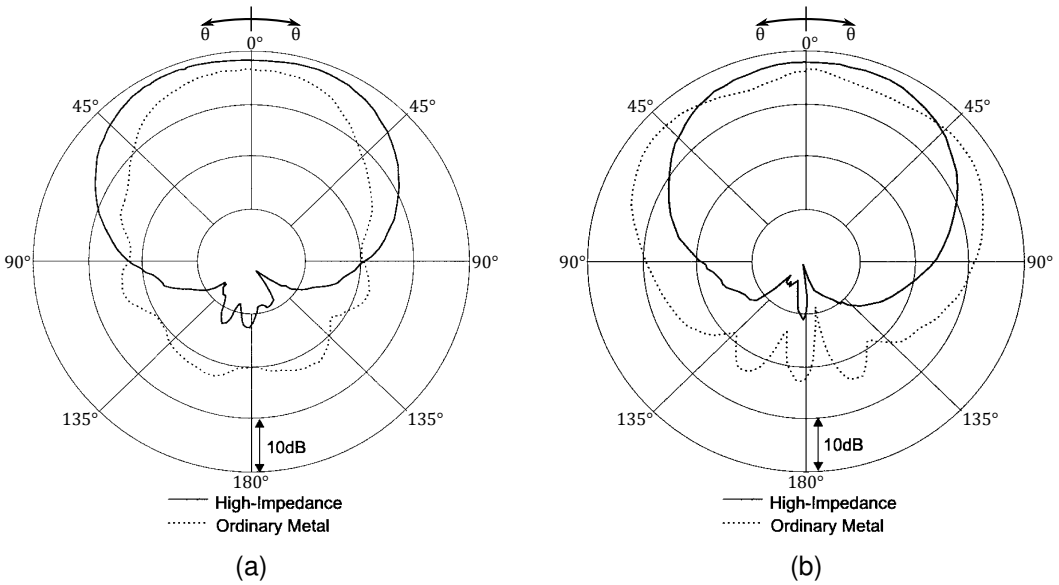

Figure 1.3: (a) H- and (b) E-plane radiation patterns of patch antennas on two different ground planes.

In Figure 1.3 is seen that for an ordinary metal plane significant radiation occurs in backward direction $90° < \theta < 180°$. The forward direction, $0° < \theta < 90°$, shows for the metal plane different behaviour in the H- and E-plane. A narrow radiation pattern in the H-plane and a broader pattern in the E-plane. The metal depends on the polarisation. This makes the radiation pattern non rotationally symmetry.
The High-impedance surface shows different behaviour. SW are not able to propagate along the surface, and no radiation occurs at the panels edge. Both planes are symmetric and the radiation patterns becomes smoother. The backward ration is almost reduced and the forward radiation improved.
Concluded SW reduction improves the radiation pattern because energy is not re-radiated any more. Panel's edges or objects in the surrounding area have less influence on the element patterns. Different radome fixation can be used or other objects can be placed closer by.

1.2.2 Surface Wave Model

In 1953, Barlow and Cullen [3] tried to create an unified picture of the theory of various kinds of existing surface waves (e.g. Zenneck Surface Waves, Sommerfeld Surface Waves, Norton Surface Waves, Harms-Goubau Axial Surface Waves [4]). Unfortunately the focus was only on propagating Transverse Magnetic (TM) SWs, by

assuming incident TM waves under one specific angle (Brewster angle). They did not give a general description of a SW. In 1960 Balow [5] came with a SW definition:

*"A **surface wave** is one that propagates along an interface between **two different media without radiation**, such radiation being construed to mean energy converted from the surface-wave field to some other form."*

This definition describes how a surface wave looks like, but it is not a mathematical description. In the coming section a SW is expressed as a mathematical expression.

A description of SW starts from Figure 1.4 and by solving Maxwell's equations in the transition region. Assume the SW propagates into the z-direction (Figure 1.4a), polarisation (Figure 1.4b independent). A general description starts from the complex plane wave solution. This means the propagation constant is complex and has an attenuation constant per unit distance depended of direction $\boldsymbol{\alpha}$, and a propagation constant, representing the change in phase per unit length depended of direction, $\boldsymbol{\beta}$. The total complex propagation constant becomes $\boldsymbol{\gamma} = \boldsymbol{\alpha} + j\boldsymbol{\beta}$. It is assumed all solutions have a time-harmonic dependency ($e^{j\omega t}$).

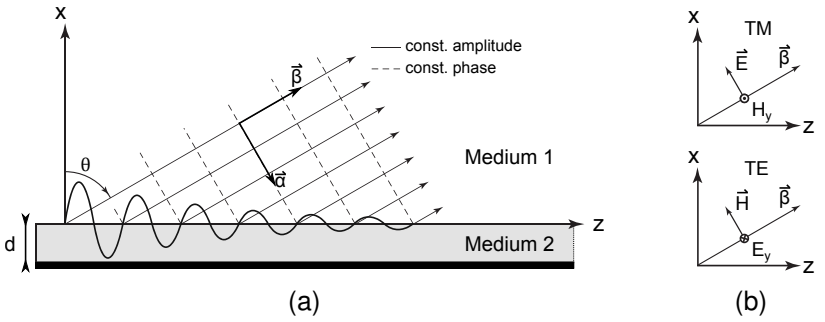

Figure 1.4: (a) General TM and TE leaky surface wave, propagating into z-direction, (b) Polarisation definition.

For now consider only the field in Medium 1 for which the electric field can be written as:

TM		TE	
$E_y = 0$	(1.4)	$E_x = E_z = 0$	(1.7)
$E_{x,z}(x,z) = E_0 e^{-\gamma_z z} e^{-\gamma_n x}$	(1.5)	$E_y = \frac{j\omega\mu_0}{\gamma_n} H_0 e^{-\gamma_z z} e^{-\gamma_n x}$	(1.8)
$= E_0 e^{-\alpha_z z - j\beta_z z} e^{-\alpha_n x - j\beta_n x}$	(1.6)	$E_y = \frac{j\omega\mu_0}{\gamma_n} H_0 e^{-\alpha_z z - j\beta_z z} e^{-\alpha_n x - j\beta_n x}$	(1.9)

where γ_z describes the propagation along the surface and γ_n the propagation normal to the surface. When $\boldsymbol{\alpha} = 0$ the amplitude stays constant for a phase front. This means a homogeneous wave or plane wave and does not take into account the

interaction with a different medium. For the opposite case, $\boldsymbol{\alpha} \neq 0$ the amplitude varies over the phase front (inhomogeneous wave, leaky wave or surface wave). Assume a TM polarization and substituting Equation 1.5 into Equation 1.10, known as Helmholtz equation, assuming free space

$$\frac{\partial^2 \boldsymbol{E}}{\partial x^2} + \frac{\partial^2 \boldsymbol{E}}{\partial y^2} + \frac{\partial^2 \boldsymbol{E}}{\partial z^2} + k_0^2 \boldsymbol{E} = 0 \tag{1.10}$$

using separation of variables [6], gives a dispersion relation:

$$\gamma_z^2 + \gamma_n^2 + \omega^2(\epsilon_0\mu_0) = 0 \tag{1.11}$$

$$\beta_z^2 + \beta_n^2 - (\alpha_z^2 + \alpha_n^2) - 2j(\alpha_z\beta_z + \alpha_n\beta_n) = \omega^2(\epsilon_0\mu_0) \tag{1.12}$$

and splitting Equation 1.12 into a real and imaginary part:

$$Re \rightarrow \beta_z^2 + \beta_n^2 - (\alpha_z^2 + \alpha_n^2) = \omega^2(\epsilon_0\mu_0) = k_0^2 \qquad \rightarrow |\boldsymbol{\beta}|^2 - |\boldsymbol{\alpha}|^2 = k_0^2 \tag{1.13a}$$

$$Im \rightarrow -2(\alpha_z\beta_z + \alpha_n\beta_n) = 0 \qquad \rightarrow \boldsymbol{\alpha} \cdot \boldsymbol{\beta} = 0 \tag{1.13b}$$

For a Plane Wave (PW) $\alpha_n = \alpha_z = 0$ and $\beta \neq 0$, and therefore only Formula 1.13a exists. On the other hand, complex travelling waves (inhomogeneous waves), have $\alpha \neq 0$ and both Formulas 1.13a and 1.13b hold.
SWs are inhomogeneous waves, $\alpha_n \neq 0$, $\alpha_z = 0$, combining with Figure 1.4a gives the components of $\boldsymbol{\alpha}$, and $\boldsymbol{\beta}$. A bounded SW has a phase constant along the surface and the attenuation constant normal to the surface pointing into the positive direction (Figure 1.5a). Unbounded waves, Leaky Waves (LWs), will 'leak' from the surface, and therefore the phase constant is pointing into free-space and has an attenuation constant pointing into the surface (Figure 1.5b). The α_n becomes negative, resulting in an infinite field in x-direction and an attenuated field into z. It is pure a theoretical description of a LW and is not possible in reality. Interchanging the α and β from the LW creates a new type of wave, known as the Zenneck SW (Figure 1.5c). This wave shows opposite behaviour compared to the LW. The wave propagates into the substrate and due to the positive α the wave shows exponential decay. In fact the Zenneck SW is a SW that decays.
All the different configurations are given in the tabular below.

Wave type	$\boldsymbol{\alpha}$	$\boldsymbol{\beta}$
PW	$\boldsymbol{\alpha} = 0$	$\boldsymbol{\beta} \neq 0$
LW	$\boldsymbol{\alpha} \neq 0$	$\boldsymbol{\beta} \neq 0$
SW	$\alpha_n \neq 0$, $\alpha_z = 0$	$\beta_n = 0$, $\beta_z \neq 0$

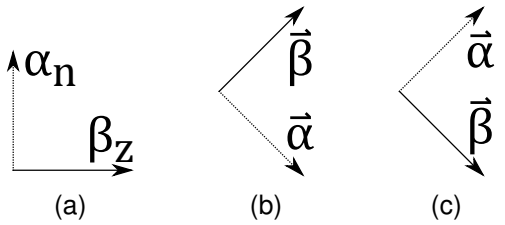

Figure 1.5: (a) Surface Wave, (b) Leaky Wave, (c) Zenneck Surface Wave.

So far, the focus was only on Medium 1 and for this layer the corresponding wave numbers were explained. But SWs, can only exists in the presence of two mediums, as part of its own definition. The combination of the field in both media determine SW propagation. Therefore the fields in Medium 2 are involved into the calculation. Solving Maxwell's equations in the transition region imposes the continuity of the tangential field components.

$$H_{1\,y} \overset{x=0}{=} H_{2\,y} \tag{1.14}$$

$$E_{1\,z} \overset{x=0}{=} E_{2\,z} \tag{1.15}$$

As consequences of the field continuity, the impedances are also equal use equal and therefore the transverse resonant condition [7] is valid. This means the situation can be modelled with an equivalent transmission line circuit, where both media are represented by a transmission line.

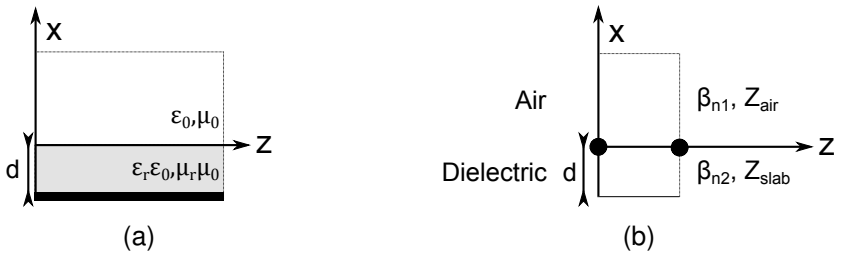

Figure 1.6: (a) $x < 0$, Dielectric slab, thickness d, and $x > 0$ air, (b) transverse resonance equivalent circuit, from Pozar [7].

The impedance sign depends on the direction of viewing ($Z_{x=0} = +$ or $-$). For example by looking towards Medium 1 from $x = 0$ gives a positive impedance, and so Medium 2 should has a negative impedance. In mathematical equations it becomes:

$$Z_{1\,x=0} = \frac{E_{1\,z}}{H_{1\,y}} \leftrightarrow \frac{E_{2\,z}}{H_{2\,y}} = -Z_{2\,x=0} \tag{1.16}$$

$$Z_{1\,x=0}(\gamma_{n\,1}) = -Z_{2\,x=0}(\gamma_{n\,2}) \tag{1.17}$$

$$Z_{1\,x=0}(\gamma_{n\,1}) + Z_{2\,x=0}(\gamma_{n\,2}) = 0 \tag{1.18}$$

The transverse resonant condition it self does not tell anything about SW propagation. For predicting SWs an additional condition is imposed from solving Maxwell's equations also known as Snell's law and is:

$$\gamma_{z\,1} = \gamma_{z\,2} \tag{1.19}$$

which links the propagation into the z-direction in both media. Whit Equations 1.17 and 1.19 a prediction can be made about SW propagation. The equations are changed by assuming SW propagation.It starts by expressing $Z_{2\,x=0}(\gamma_z)$ in Equation 1.17 to a propagation constant in z-direction. Equation 1.11 is used for this propagation transformation but with the corresponding materials properties and becomes:

$$\gamma_z^2 + \gamma_n^2 + \mu_r \epsilon_r k_0^2 = 0 \tag{1.20}$$

Furthermore the impedance of medium 1 (air) is known and so Equation 1.17 can be rewritten to:

$$\gamma_{n\,1} = Z_{2\,x=0}(\gamma_{z\,2}; freq) \tag{1.21}$$

Equation 1.20 is used again for expressing $\gamma_{n\,1}$ towards $\gamma_{z\,1}$ ($\mu_r = \epsilon_r = 0$):

$$\gamma_{z\,1} = \sqrt{k_0^2 - \gamma_{n\,1}^2}\gamma_{z\,1} = \sqrt{k_0^2 - \left(Z_{2\,x=0}(\gamma_{z\,2}; freq)\right)^2} \tag{1.22}$$

This function shows a function where $\gamma_{z\,1}$ depends on $\gamma_{z\,2}$. However according Equation 1.19 these propagation constants are equal. When these equations are solved graphically, both equations are plotted in the same figure (Figure 1.7). If a SW exists there is one point where these equations are equal: the intersection point. Figure 1.7 shows this intersection for real propagation constants for one particular frequency. Changing the frequency gives different intersections and reveals a dispersion diagram. More information and an example is given in Subsection 2.1.1.

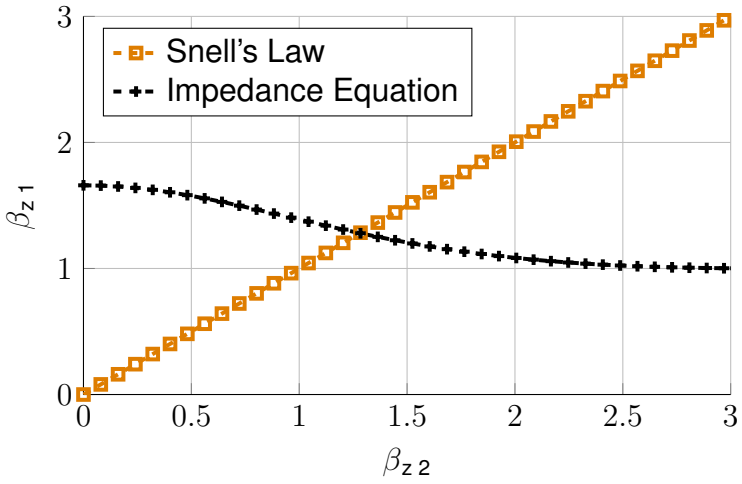

Figure 1.7: Plotted dispersion equations for one frequency.

1.2.3 Surface Waves Reduction

In order to modify or attenuate SW propagation, the SW should be expressed in both mediums by using the transverse resonant conditions. For using the transverse resonant condition, Equation 1.18, the impedances of both mediums should be known. Medium 1 is assumed to be air and the impedance is derived in Appendix A for both polarizations and replace β_n with a complex propagation constant $-j\gamma_n$, where $\gamma_n = \alpha_n + j\beta_n$, for angle of incidence and independent of polarisation. According to Figure 1.8 a SW propagates into z and so $\beta_n = 0$.

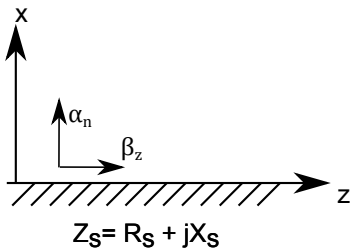

Figure 1.8: Illustration of a plane impedance surface, with propagating SW.

The other Medium, Medium 2, can be a dielectric slab, a periodic complicated structure, as long as the period is small compared to the wavelength, or any other material. In these cases the surface is approachable by an equivalent surface impedance, $Z_s = R_s + jX_s$. Furthermore the assumption is made that Medium 2 is independent of polarisation or angle of incident.

The found impedances are used in the transverse resonant equation for both polarisations. The impedances is inspected from $x = 0$ towards the positive side.

$$
\begin{aligned}
Z_{TM\,air} &= \frac{-j\gamma_n}{\omega\epsilon_0} \\
&\overset{SW}{\rightarrow} \frac{-j\alpha_{n\,1}}{\omega\epsilon_0}
\end{aligned} \tag{1.23}
$$

$$
\begin{aligned}
Z_{TE\,air} &= \frac{\omega\mu_0}{-j\gamma_n} = \omega\mu_0\frac{(\beta_{n\,1} + j\alpha_{n\,1})}{\beta_{n\,1}^2 + \alpha_{n\,1}^2} \\
&\overset{SW}{\rightarrow} \frac{j\omega\mu_0}{\alpha_{n\,1}}
\end{aligned} \tag{1.24}
$$

Substituting Equation 1.23 and Equation 1.24 in Equation 1.18, and assuming $Z_{s\,n} = R_s + jX_s$.

$$
\begin{aligned}
Z_{TM} &= -Z_s^{TM} \\
\frac{-j\alpha_{n\,1}}{\omega\epsilon_0} &= -Z_s = -R_s - jX_s
\end{aligned} \tag{1.25}
$$

$$
\begin{aligned}
Z_{TE} &= -Z_s^{TE} \\
\frac{j\omega\mu_0}{\alpha_{n\,1}} &= -Z_s = -R_s - jX_s
\end{aligned} \tag{1.26}
$$

From both equations, Equation 1.25 and Equation 1.26 is concluded that changing the imaginary part controls the normal attenuation constant, or in other words it determines how closely the SW is bound to the surface. Furthermore from these two equations it is seen that the sign of the imaginary part also contains SW propagation information. Equation 1.25 shows that for TM SW propagation the imaginary part should be positive. In contrast to Equation 1.26 that shows for TE SW propagation the imaginary part should be negative.

The propagation into z-direction is calculated from Equations 1.23 and 1.24 in combination with the wave number equation:

$$
k_0^2 = \gamma_{n\,1}^2 + \gamma_{z\,1}^2 \tag{1.27}
$$

where $\boldsymbol{\gamma} = -j\,(\boldsymbol{\alpha} + j\boldsymbol{\beta})$. For a pure SW the complex propagation constant into z-direction only depends on β_z and $\alpha = 0$ and so the propagation into z-direction becomes:

$$-j\alpha_{z1TM} + \beta_{z1TM} = \sqrt{k_0^2 - \omega^2\epsilon_0^2\left(R_s^2 - X_s^2 + 2R_sX_sj\right)} \tag{1.28}$$

$$\beta_{z1TM} \overset{SW}{=} \sqrt{k_0^2 - \omega^2\epsilon_0^2\left(R_s^2 - X_s^2\right)} \tag{1.29}$$

$$-j\alpha_{z1TE} + \beta_{z1TE} = \sqrt{k_0^2 + \frac{\omega^2\mu_0^2}{R_s^2 - X_s^2 + 2R_sX_sj}} \tag{1.30}$$

$$\beta_{z1TE} \overset{SW}{=} \sqrt{k_0^2 + \frac{\omega^2\mu_0^2}{R_s^2 - X_s^2}} \tag{1.31}$$

The β_z component is linked to the relation $R_s^2 - X_s^2$. When $R_s < X_s$, β_z is real and therefore the wave is bound to the surface. In the other scenario, when $R_s > X_s$, β_z becomes imaginary and the wave propagates away from the surface (leaky wave).

For TM waves the same conclusion is found by Collin [8]. He assumes a normalized surface impedance with respect to the intrinsic impedance Z_0. Furthermore he investigated only TM polarisation since naturally occurring surfaces have an inductive reactive term in the surface impedance. Hence, TM surface waves are more common than TE SWs. His explanation is used to create a graphical representation, starting from an incident TM wave, Figure 1.9. From the resulting figures it can be seen what the effect is of the surface impedance on the SW propagation.

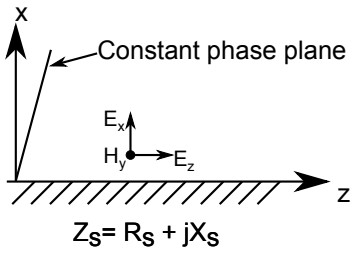

Figure 1.9: Illustration of a plane impedance surface, with a TM surface wave.

The magnetic field in the top part ($x > 0$) is expressed as:

$$H_y = Ae^{(j\gamma_n x - j\gamma_z z)} \tag{1.32}$$

where $\gamma_n^2 + \gamma_z^2 = k_0^2$ and the electric field components are given by:

$$j\omega\epsilon_0 E_z = \frac{\partial H_y}{\partial x} \tag{1.33}$$

$$j\omega\epsilon_0 E_x = -\frac{\partial H_y}{\partial z} \tag{1.34}$$

and from which the wave impedance is found:

$$Z_{TM} = \frac{E_Z}{H_y} = \frac{\gamma_n}{\omega\epsilon_0} = \frac{\gamma_n}{k_0}Z_0 \tag{1.35}$$

By using the transverse resonant condition he find the same surface wave dependency as function of the surface impedance.
In Figure 1.10 the magnetic field component is inspected for different surface impedances.

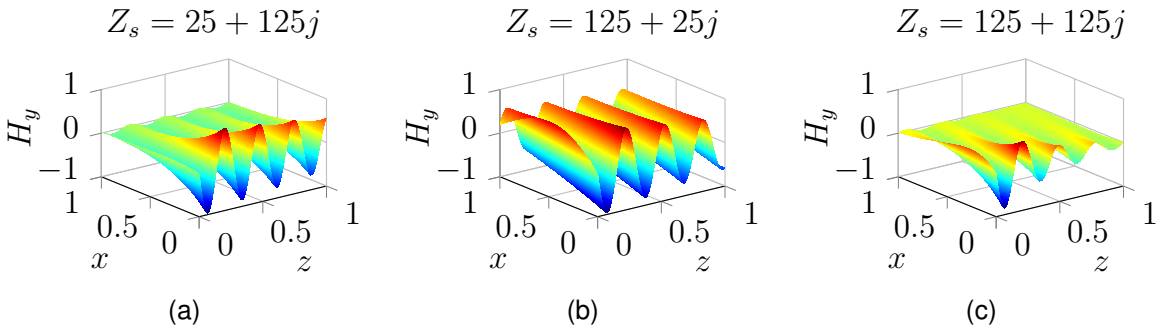

Figure 1.10: Different surface impedances and the impact on a TM propagating SW.

The first conclusion from Figure 1.10 is that a positive imaginary part supports a TM SW. The same was predicted with Equation 1.25.
Furthermore when Figure 1.10a is compared to Figure 1.10b it is noticed that fore a bound SW should hold $R_s < X_s$. This was already found by using Equation 1.29.
In Figure 1.10c an attenuated SW is shown. This can not explained by neither Equation 1.25 nor Equation 1.29 because the assumption was made a pure SW is present. For an attenuated SW an attention factor is needed and Equation 1.28 should be used. The product $R_s X_s$ determines the attenuation. For Figure 1.10c the product is larger compared to Figure 1.10a and Figure 1.10b. This means the wave is more attenuated. In addition Figure 1.10c shows $R_s = X_s$. From the colour it is seen that H_y is stronger at $x = 1, y = 0$ and $z = 0$ compared to Figure 1.10a where $R_s < X_s$. This means a small part radiates from the surface.

Concluded changing the surface impedance affects the propagation properties. For SW reduction the surface should have a high real part and a small imaginary part and/or the product $R_s X_s$ should be large. Although increasing the real part might be a proper solution, it is better to change the imaginary part. The real part absorbs the wave's energy, which results into head at unwanted places. Furthermore the transmitted signal is produced with a lot of costly components and energy absorbing is waste of energy. Changing the imaginary part effects the bounding conditions. A lossless bounded SW propagates into free space and it is the preferred method.
Changing the imaginary part only, is not straightforward. A metallized surface has a surface impedance [8]:

$$Z_s = Z_0(1+j)\sqrt{\frac{\gamma_0}{2\sigma Z_0}} \tag{1.36}$$

where the real part can not be changed independent of the imaginary part. Furthermore σ is for metals large (order of 10^7 [9]) and so the real and imaginary parts are small, leading to a unbound, less attenuated TM SW.
Another possibility is a grounded dielectric surface. The surface impedance are derived in Appendix A and the results is given below:

$$Z_{sTM} = \frac{\gamma_{n\,2}}{\omega\epsilon_r\epsilon_0} j \tan\left(\gamma_{n\,2} d\right) \tag{1.37}$$

$$Z_{sTE} = \frac{\omega\mu_r\mu_0}{\gamma_{n\,2}} j \tan\left(\gamma_{n\,2} d\right) \tag{1.38}$$

where d is the substrate's thickness. The $\tan$ functions is responsible for a flipping sign as function of frequency and the substrate's thickness, supporting TM and TE SWs. Yakovlev *et al.* [10] derived a frequency-wavenumber diagram, also known as dispersion diagram. Such diagram shows for which frequency propagation is possible. The used slab thickness is 1 mm and a permittivity is used of $\epsilon = 10.2$. The found dispersion diagram is shown in Figure 1.11. For every wavenumber there exists a frequency and so SWs are always present.

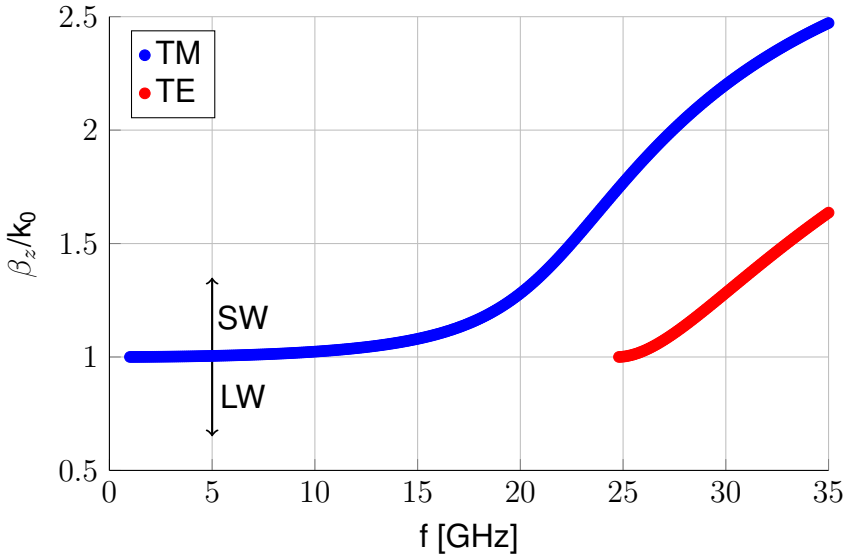

Figure 1.11: Dispersion diagram for a grounded dielectric slab. Design is created by Luukkonen *et al.* [11].

All modes in Figure 1.11 start from $\beta_z/k_0 > 1$. The reason for this is the SW assumption, the wave decays exponentially into the normal direction. This is only possible for β_n values that are imaginary:

$$\beta_n = k_0\sqrt{1 - \beta_z^2/k_0^2} \tag{1.39}$$

Cases where $\beta_z/k_0 < 1$ do exist, known as LW. In Subsection 3.2.4 LWs are shortly addressed but this area does not belong to the major area of interest.
Unfortunately, the current surfaces do not contain a region where no SW can propagate. Especially this kind of behaviour is wanted. In literature different examples can be found for changing the surface impedance:

- Corrugations: varying thickness and material properties of a grounded dielectric slab. When the thickness is changed many times within a period p ($p << \lambda$) the surface can be represented with a surface impedance and is known as a corrugated surface [3], [12]–[15]. Also variations are possible where the corrugation behaves like a cavity [16].
- Placing hemispherical structures on top of the surface. The radius and spacing between the centres are small compared to the wavelength. These structures are made from a different material (ϵ, μ, σ) and are uniform distributed on a conducting surface [17]
- Electromagnetic Band Gap (EBG) surfaces also known as Frequency-Selective Surfaces (FSS) that form High-Impedance Surface (HIS) [18], [19]. These structures can be placed in one plane (xy-plane, uniplanar) or in multiple planes (xy,xz planes, multiplanair). A broad variety is available for uniplanar structures starting from metallic uniform lines to more complicated structures [20]–[23]. Also many structures are known for multiplanar configurations [24]–[27] but are a variation of the well known mushroom structures invented by Sievenpiper [28].

Especially the last one, EBG surfaces, is the preferred method because: firstly, the fabrication steps can easily be included into current Printed Circuit Board (PCB) fabrication steps. Secondly, the antenna panel remains perfectly flat, and last, the thickness/height needed to be effective is less compared to a corrugated surface ($^{\lambda}/_{2}$).
Therefore this investigation focuses on changing the surface impedance by placing structures in/on top of the surface. Although uniplanar structures show band gap regions, multiplanar structures show a larger bandwidth for the band gap [29] and so these structures are preferred.
In general multiplanar structures are easier to model compared to uniplanar structures. Multiplaner structures are formed by multiple planes and each individual plane can be calculated. Within this thesis multiplanar structures are investigated and especially the Sievenpipers mushroom structures (Figure 1.12).

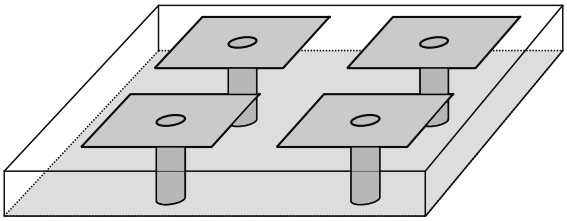

Figure 1.12: Sievenpiper mushroom structure, integrated into a grounded dielectric slab, metal parts are coloured grey.

Sievenpiper *et al.* [2] described the mushroom structure with a capacitor and an inductor shown in Figure 1.13a and derived a simple impedance equation:

$$Z = \frac{j\omega L}{1 - \omega^2 LC} \tag{1.40}$$

The surface is inductive at low frequencies and capacitive at high frequencies and gives a resonant frequency:

$$\omega_0 = \frac{1}{\sqrt{LC}} \tag{1.41}$$

and by inspecting the reflection phase shift for different frequencies reveal the surface behaviour, shown in Figure 1.13b.

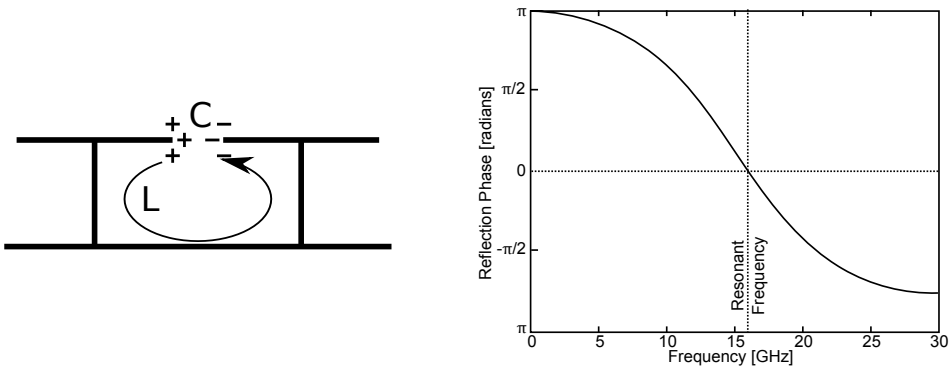

(a) (b)

Figure 1.13: (a) Sievenpiper mushroom representation, (b) reflection phase of the high-impedance surface [2].

Different models are available that describe mushroom structures and there corresponding effective surface impedance. All the models related the frequency to the corresponding wave number and so it reveals the wave propagation properties into a specific direction (dispersion diagram). The models are:

- Sievenpiper representation, shown above (Figure 1.12). He represents mushrooms as lumped components seen from the dielectric layer. Further research

extend this idea to periodic structures, for example research done by Rahman and Stuchly [30] and Caloz and Itoh [31]. They use a different name for their models known as Composite Right/Left-Handed (CRLH) Transmission Line (TL) model.

- Impedance representation of each individual layer. A total surface impedance is created by the combination of each individual impedance representation. Yakovlev *et al.* [10] explain this method. This method is known in this thesis as Coupled Free-Space - Surface IMpedance (COF-SIM) TL model.
- Full wave electromagnetic simulations with a software suite like Ansys High Frequency Structure Simulator (HFSS). The possibilities of SW prediction are shown by Raza [32].

1.3 Investigation Goals

The goal of this investigation is to find out how SWs can be reduced using the mushroom structure. Different theoretical models are investigated and validated using Ansys HFSS simulations. One of the theoretical models is used to design a mushroom that has band gap in the wanted region. Furthermore, having a proper design, the structure is investigated in two scenarios. In the first scenario the mushrooms are placed in between the patch antennae to find out if the mutual coupling is effected. The second scenario is when the structure is placed in the available free space, that is formed by the outer row of the array antenna and the antenna panel's edge.

1.4 Report organization

In this section, the introduction, the basic aspects of SWs were addressed as well as their reduction using mushrooms structures. Chapter 2 addresses the mushroom with (detailed) models: the COF-SIM TL model is explained in Subsection 2.1, CRLH TL model is addressed in Subsection 2.2 and last the HFSS simulation is discussed in Subsection 2.3. The COF-SIM model is used to design a mushroom where the band gap occurs in the wanted region. These results are compared to the CRLH TL model and HFSS simulations (Chapter 3). So far the structure is only investigated as a single element, in Chapter 4 the extension is made to multiple mushrooms to inspect mutual coupling behaviour and edge re-radiation. The report ends with the conclusions and recommendations (Chapter 5).

Chapter 2

Reducing Surface Waves; a Theoretical Approach

Not publicly accessible, only chapter names are given.

2.1 Coupled Free-Space - Surface Impedance TL Model

2.1.1 Air-Grounded Dielectric Slab

Dispersion Equation

2.1.2 Air-Patch-Grounded Dielectric Substrate

β_z Direction Limitations

Impedance: Grid

Dispersion Equation

2.1.3 Air-Patch-Via-Grounded Dielectric Substrate

Directional Permittivity

Modelling Directive Permittivity ϵ_{xx}

Vias Frequency Dependency

Via Medium Impedance

Dispersion Equation

2.2 Composite Right/Left-Handed TL Model

2.2.1 1-D CRLH $\Delta z \to 0$

2.2.2 1-D CRLH $\Delta z \to D$

2.3 HFSS Eigenmode Solver

2.3.1 HFSS Limitations

Chapter 3

EBG Concept Design and Validation Theoretical Models

3.1 EBG Concept Design

3.2 Validation Theoretical Models

3.2.1 HFSS Eigenmode Solver

HFSS Eigenmode Settings

Transition Region

3.2.2 COF-SIM TL Model - HFSS Eigenmode Comparison

3.2.3 CRLH TL Model - HFSS Eigenmode Comparison

3.2.4 Leaky Wave Region Investigation

Chapter 4

Reducing Surface Waves; a Practical Environment

4.1 Mutual Coupling Reduction Between Antenna Elements

4.1.1 HFSS MC Simulation Model

4.1.2 HFSS MC Results

4.2 Edge Surface Wave Reduction

4.2.1 TM Waves and Edge SW Reduction

4.2.2 TE Waves and Edge SW Reduction

4.2.3 Edge SW Reduction Conclusion

Chapter 5

Conclusions and Recommendations

5.1 Conclusions

5.2 Recommendations

Bibliography

[1] C. A. Balanis, *Antenna theory: analysis and design*, 3rd ed. John Wiley & Sons, 2005, ch. 6, pp. 290–296.

[2] D. Sievenpiper, L. Zhang, R. F. J. Broas, N. G. Alexopolous, and E. Yablonovitch, "High-impedance electromagnetic surfaces with a forbidden frequency band," *IEEE Transactions on Microwave Theory and Techniques*, vol. 47, no. 11, pp. 2059–2074, Nov 1999.

[3] H. M. Barlow and A. L. Cullen, "Surface waves," *Proceedings of the IEE - Part III: Radio and Communication Engineering*, vol. 100, no. 68, pp. 329–341, November 1953.

[4] S. Schelkunoff, "Anatomy of "surface waves"," *IRE Transactions on Antennas and Propagation*, vol. 7, no. 5, pp. 133–139, December 1959.

[5] H. E. M. Barlow, "Surface waves: a proposed definition," *Proceedings of the IEE - Part B: Electronic and Communication Engineering*, vol. 107, no. 33, pp. 240–, May 1960.

[6] D. Pozar, *Microwave Engineering*, 4th ed. Wiley, 2011, ch. 1, pp. 20–23.

[7] ——, *Microwave Engineering*, 4th ed. Wiley, 2011, ch. 3, pp. 153–154.

[8] R. Collin, I. Antennas, and P. Society, *Field theory of guided waves*, ser. The IEEE/OUP Series on Electromagnetic Wave Theory (Formerly IEEE Only), Series Editor Series. IEEE Press, 1991, ch. Surface Waveguides, pp. 697–708.

[9] C. A. Balanis, *Advanced engineering electromagnetics*. John Wiley & Sons, 1989.

[10] A. B. Yakovlev, M. G. Silveirinha, O. Luukkonen, C. R. Simovski, I. S. Nefedov, and S. A. Tretyakov, "Characterization of surface-wave and leaky-wave propagation on wire-medium slabs and mushroom structures based on local and nonlocal homogenization models," *IEEE Transactions on Microwave Theory and Techniques*, vol. 57, no. 11, pp. 2700–2714, Nov 2009.

[11] O. Luukkonen, A. B. Yakovlev, C. R. Simovski, and S. A. Tretyakov, "Comparative study of surface waves on high-impedance surfaces with and without vias," in *2008 IEEE Antennas and Propagation Society International Symposium*, July 2008, pp. 1–4.

[12] A. F. Harvey, "Periodic and guiding structures at microwave frequencies," *IRE Transactions on Microwave Theory and Techniques*, vol. 8, no. 1, pp. 30–61, January 1960.

[13] M. N. M. Kehn, "Rapid surface-wave dispersion and plane-wave reflection analyses of planar corrugated surfaces by asymptotic corrugations boundary conditions even for oblique azimuth planes," *IEEE Transactions on Antennas and Propagation*, vol. 61, no. 5, pp. 2695–2707, May 2013.

[14] C. Mentzer and L. Peters, "Properties of cutoff corrugated surfaces for corrugated horn design," *IEEE Transactions on Antennas and Propagation*, vol. 22, no. 2, pp. 191–196, Mar 1974.

[15] R. Elliott, "On the theory of corrugated plane surfaces," *Transactions of the IRE Professional Group on Antennas and Propagation*, vol. 2, no. 2, pp. 71–81, Apr 1954.

[16] C. Molero, R. Rodriguez-Berral, F. Mesa, and F. Medina, "Analytical circuit model for 1-d periodic t-shaped corrugated surfaces," *IEEE Transactions on Antennas and Propagation*, vol. 62, no. 2, pp. 794–803, Feb 2014.

[17] J. Wait, "Guiding of electromagnetic waves by uniformly rough surfaces : Part i," *IRE Transactions on Antennas and Propagation*, vol. 7, no. 5, pp. 154–162, December 1959.

[18] F. Yang and Y. Rahmat-Samii, *Electromagnetic band gap structures in antenna engineering*. Cambridge university press Cambridge, UK, 2009.

[19] R. Garg, P. Bhartia, I. Bahl, and A. Ittipiboon, *Microstrip antenna handbook*, 2001.

[20] S. Keyrouz, G. Perotto, and H. J. Visser, "Lumped-elements tunable frequency selective surfaces," in *The 8th European Conference on Antennas and Propagation (EuCAP 2014)*, April 2014, pp. 475–478.

[21] F. Costa, S. Genovesi, A. Monorchio, and G. Manara, "A circuit-based model for the interpretation of perfect metamaterial absorbers," *IEEE Transactions on Antennas and Propagation*, vol. 61, no. 3, pp. 1201–1209, March 2013.

[22] B. A. Munk, *Finite antenna arrays and FSS*. John Wiley & Sons, 2003.

[23] ——, *Frequency Selective Surfaces: Theory and Design*. Wiley Online Library, 2000.

[24] H. N. B. Phuong, H. V. Phi, N. K. Kiem, D. N. Dinh, T. M. Tuan, and D. N. Chien, "Design of compact ebg structure for array antenna application," in *2015 International Conference on Advanced Technologies for Communications (ATC)*, Oct 2015, pp. 178–182.

[25] C. B. Mulenga and J. A. Flint, "Planar electromagnetic bandgap structures based on polar curves and mapping functions," *IEEE Transactions on Antennas and Propagation*, vol. 58, no. 3, pp. 790–797, March 2010.

[26] D. H. Margaret, M. R. Subasree, S. Susithra, S. S. Keerthika, and B. Manimegalai, "Comparison of compact ebg structures on the mutual coupling reduction of antenna arrays," *International Journal of Future Computer and Communication*, vol. 3, no. 2, pp. 76–79, 2014.

[27] L. Peng, C. l. Ruan, and J. Xiong, "Compact ebg for multi-band applications," *IEEE Transactions on Antennas and Propagation*, vol. 60, no. 9, pp. 4440–4444, Sept 2012.

[28] D. Sievenpiper, "High-impedance electromagnetic surfaces," Ph.D. dissertation, University of California, 1991.

[29] F. Yang and Y. Rahmat-Samii, *Electromagnetic band gap structures in antenna engineering*. Cambridge university press Cambridge, UK, 2009.

[30] M. Rahman and M. A. Stuchly, "Transmission lineâĂŞperiodic circuit representation of planar microwave photonic bandgap structures," *Microwave and Optical Technology Letters*, vol. 30, no. 1, pp. 15–19, 2001.

[31] C. Caloz and T. Itoh, *Electromagnetic Metamaterials: Transmission Line Theory and Microwave Applications*. John Wiley & Sons, 2005.

[32] S. Raza, "Characterization of the reflection and dispersion properties of 'mushroom'-related structures and their application to antennas," Master's thesis, University of Toronto, 2012.

[33] A. Lai, "Left-handed metamaterials for microwave engineering applications," Application Workshops for High-Performance Electronic Design, department of Electrical Engineering, University of California.

[34] S. Keyrouz, G. Perotto, and H. J. Visser, “Lumped-elements tunable frequency selective surfaces,” in *The 8th European Conference on Antennas and Propagation (EuCAP 2014)*, April 2014, pp. 475–478.

[35] R. J. Langley and E. A. Parker, “Equivalent circuit model for arrays of square loops,” *Electronics Letters*, vol. 18, no. 7, pp. 294–296, April 1982.

[36] C. K. Lee and R. J. Langley, “Equivalent-circuit models for frequency-selective surfaces at oblique angles of incidence,” *IEE Proceedings H - Microwaves, Antennas and Propagation*, vol. 132, no. 6, pp. 395–399, October 1985.

[37] J. R. Wait, “Reflection at arbitrary incidence from a parallel wire grid,” *Applied Scientific Research, Section A*, vol. 4, no. 1, pp. 393–400, 1955.

[38] N. Marcuvitz and I. of Electrical Engineers, “Waveguide handbook,” ser. Electromagnetics and Radar Series. P. Peregrinus, 1951, pp. 280–285.

[39] J. D. Joannopoulos, R. D. Meade, and J. N. Winn, *Photonic Crystals: Molding the Flow of Light*. Princeton University Press, 1995, ch. Appendix B, pp. 112–120.

[40] O. Luukkonen, C. Simovski, G. Granet, G. Goussetis, D. Lioubtchenko, A. V. Raisanen, and S. A. Tretyakov, “Simple and accurate analytical model of planar grids and high-impedance surfaces comprising metal strips or patches,” *IEEE Transactions on Antennas and Propagation*, vol. 56, no. 6, pp. 1624–1632, June 2008.

[41] F. Costa, A. Monorchio, and G. Manara, “Efficient analysis of frequency-selective surfaces by a simple equivalent-circuit model,” *IEEE Antennas and Propagation Magazine*, vol. 54, no. 4, pp. 35–48, Aug 2012.

[42] O. Luukkonen, C. R. Simovski, A. V. Raisanen, and S. A. Tretyakov, “An efficient and simple analytical model for analysis of propagation properties in impedance waveguides,” *IEEE Transactions on Microwave Theory and Techniques*, vol. 56, no. 7, pp. 1624–1632, July 2008.

[43] O. Luukkonen, F. Costa, C. R. Simovski, A. Monorchio, and S. A. Tretyakov, “A thin electromagnetic absorber for wide incidence angles and both polarizations,” *IEEE Transactions on Antennas and Propagation*, vol. 57, no. 10, pp. 3119–3125, Oct 2009.

[44] J. B. Pendry, A. J. Holden, W. J. Stewart, and I. Youngs, “Extremely low frequency plasmons in metallic mesostructures,” *Phys. Rev. Lett.*, vol. 76, pp. 4773–4776, Jun 1996.

[45] S. Tretyakov, *Analytical Modeling in Applied Electromagnetics*, ser. Artech House electromagnetic analysis series. Artech House, 2003, ch. 5, pp. 164–179.

[46] P. A. Belov, R. Marques, S. I. Maslovski, I. S. Nefedov, M. Silveirinha, C. R. Simovski, and S. A. Tretyakov, "Strong spatial dispersion in wire media in the very large wavelength limit," *Phys. Rev. B*, vol. 67, p. 113103, Mar 2003.

[47] E. Hecht, *Optics Third Edition*, 3rd ed. Addison-Wesley, 1998, ch. 4, pp. 127 – 129.

[48] T. Bastian, "Notes on electromagnetic waves in plasma," class notes for Computational Mechanics, National Radio Astronomy Observatory, Charlottesville, VA, December 2005.

[49] J. D. Joannopoulos, R. D. Meade, and J. N. Winn, *Photonic Crystals: Molding the Flow of Light*. Princeton University Press, 1995, ch. 3, pp. 28–31.

[50] S. Tretyakov, *Analytical Modeling in Applied Electromagnetics*, ser. Artech House electromagnetic analysis series. Artech House, 2003, ch. 4, pp. 70–74.

[51] R. King, D. Thiel, and K. Park, "The synthesis of surface reactance using an artificial dielectric," *IEEE Transactions on Antennas and Propagation*, vol. 31, no. 3, pp. 471–476, May 1983.

[52] G. V. Eleftheriades, A. K. Iyer, and P. C. Kremer, "Planar negative refractive index media using periodically l-c loaded transmission lines," *IEEE Transactions on Microwave Theory and Techniques*, vol. 50, no. 12, pp. 2702–2712, Dec 2002.

[53] N. Engheta and R. W. Ziolkowski, *Metamaterials: physics and engineering explorations*. John Wiley & Sons, 2006.

[54] M. Maasch, *Tunable Microwave Metamaterial Structures*. Springer, 2016.

[55] C. Caloz and T. Itoh, *Electromagnetic metamaterials: transmission line theory and microwave applications*. John Wiley & Sons, 2005, ch. 3, pp. 59–74.

[56] ——, *Electromagnetic metamaterials: transmission line theory and microwave applications*. John Wiley & Sons, 2005, ch. 2, pp. 28–37.

[57] D. Pozar, *Microwave Engineering*, 4th ed. Wiley, 2011, ch. 8, pp. 380–388.

[58] *Left-Handed Metamaterial Design Guide*, Ansoft Corporation, 2007.

[59] D. R. Jackson, J. T. Williams, A. K. Bhattacharyya, R. L. Smith, S. J. Buchheit, and S. A. Long, "Microstrip patch designs that do not excite surface waves," *IEEE Transactions on Antennas and Propagation*, vol. 41, no. 8, pp. 1026–1037, Aug 1993.

[60] D. Pozar, *Microwave Engineering*, 4th ed. Wiley, 2011, ch. 3, pp. 95–101.

[61] C. A. Balanis, *Antenna theory: analysis and design*, 3rd ed. John Wiley & Sons, 2005, ch. 12, pp. 703–707.

[62] D. Pozar, *Microwave Engineering*, 4th ed. Wiley, 2011, ch. 4, pp. 188–194.

Appendix A

Derivation Directional Impedance for Via Medium

Appendix B

Derivation Valid Regions COF-SIM Model

Appendix C

Notes on HFSS Eigenmode Solver

C.1 Height Variation

C.2 Mode Inspection

Appendix D

HFSS Model Composite Right/Left-Handed Model

Appendix E

Reducing Surface Waves; a Practical Environment, extending plots

E.1 0.8 f/f_n

TM

TE

E.2 1.1 f/f_n

TM

TE

E.3 1.3 f/f_n

TM

TE

E.4 TE Electric Vector Field plot

E.4.1 0.8 f/f_n

E.4.2 1.1 f/f_n

E.4.3 1.3 f/f_n